Capturing fleeting intermediates in a catalytic C–H amination reaction cycle

Richard H. Perry[1], Thomas J. Cahill III[1], Jennifer L. Roizen, Justin Du Bois[2], and Richard N. Zare[2]

Department of Chemistry, Stanford University, Stanford, CA 94305-5080

Edited* by Robert G. Bergman, University of California, Berkeley, CA, and approved September 21, 2012 (received for review May 4, 2012)

We have applied an ambient ionization technique, desorption electrospray ionization MS, to identify transient reactive species of an archetypal C–H amination reaction catalyzed by a dirhodium tetracarboxylate complex. Using this analytical method, we have detected previously proposed short-lived reaction intermediates, including two nitrenoid complexes that differ in oxidation state. Our findings suggest that an Rh-nitrene oxidant can react with hydrocarbon substrates through a hydrogen atom abstraction pathway and raise the intriguing possibility that two catalytic C–H amination pathways may be operative in a typical bulk solution reaction. As highlighted by these results, desorption electrospray ionization MS should have broad applicability for the mechanistic study of catalytic processes.

mass spectrometry | transient intermediates | C–H oxidation | catalysis

Catalytic methods for selective C–H oxidation rely on the exquisite choreography of a series of ligand substitution and redox events (1, 2) and in some instances, the controlled generation of a hyperreactive electrophile (3–5). The Du Bois laboratory has developed an amination protocol that uses the catalyst bis [rhodium(α,α,α′,α′-tetramethyl-1,3-benzenedipropionic acid)], hereafter designated as $Rh_2(esp)_2$, to promote both intra- and intermolecular oxidation reactions (1, 2). Indirect evidence has implicated a reactive Rh-nitrene intermediate that oxidizes saturated C–H bonds through a concerted asynchronous two-electron insertion event (6–10). Studies of the reaction mechanism suggest the generation of a one-electron oxidized form of the catalyst, $[Rh_2(esp)_2]^+$, which appears to result from reaction of the nitrenoid oxidant (4, 5, 11). The fast rates of the on- and off-path steps in this catalytic process and the transient nature of the reactive Rh-nitrene have confounded direct detection of many of the proposed reaction intermediates.

A preponderance of experimental and theoretical data (7–10, 12, 13) supports the mechanism for Rh-catalyzed C–H amination depicted in Fig. 1. Sulfamate **2** and iodine oxidant **3** condense to form iminoiodinane **4** (14, 15). The iminoiodinane is a ligand for $Rh_2(esp)_2$, which react to generate $[Rh_2(esp)_2]$•$PhINSO_2OR$ **5**; subsequent loss of iodobenzene (PhI) furnishes nitrenoid **6**. Oxidation of adamantane by **6** gives the sulfonamide product **7** and regenerates the dirhodium catalyst **1**. The structures of intermediates **5** and **6** were postulated through analogy to carbenoid intermediates in reactions of dirhodium catalysts with diazo compounds, and to the best of our knowledge, have not been observed spectroscopically (6–10, 12, 13). In our experience, the oxidation of substrate by Rh-nitrene **6** seems to correlate with competitive formation of a mixed-valent (Rh^{2+}/Rh^{3+}) dimer **8** that visibly colors the reaction solution red. Previous studies show that this red species is generated when $Rh_2(esp)_2$ **1**, sulfamate **2**, and oxidant **3** are mixed in solution (e.g., 0.3 mM **1** in chlorobenzene) (4, 5, 11). In this report, we provide direct evidence for the formation of species **8**.

The Zare laboratory has recently shown that desorption electrospray ionization (DESI) (16–19) coupled to MS can identify fleeting reaction intermediates having lifetimes on the order of milliseconds or less (20–22). In a DESI-MS experiment (Fig. 2), charged or neutral droplets in a stream of gas form a spray that impacts a surface containing a sample of interest and extracts analyte into secondary microdroplets. Subsequent desolvation generates gas-phase ions that can be mass analyzed (16–21). By coupling DESI to a high-resolution Orbitrap mass spectrometer (23, 24), we are able to detect transient species with high mass accuracy (1 to 5 ppm). In this study, we performed C–H amination experiments by spraying a solution of the sulfamate ester **2** ($ROSO_2NH_2$; R = CH_2CCl_3) and iodine(III) oxidant **3** at $Rh_2(esp)_2$ **1** or a mixture of **1** and a hydrocarbon substrate (adamantane) deposited on a paper surface (Fig. 2). This analytical method (20–22, 25–28) provides direct evidence for Rh-nitrene formation and the ability of this two-electron oxidant to react through hydrogen atom abstraction. Previous studies using computational and spectroscopic methods estimate that the nitrenoid species has a half-life in the nanosecond to microsecond regime (29–32), underscoring the impressive capabilities of DESI-MS to capture transient intermediates in solution-phase catalytic cycles of complex reactions. It should be recognized, however, that this mass spectrometric study identifies numerous transient species, but does not explicitly establish the kinetic competency of a particular species on the reaction coordinate.

Results and Discussion

Initial experiments were performed to establish the viability of generating amination product **7** under a standard DESI-MS protocol. A solution of trichloroethylsulfamate **2** [$Cl_3CCH_2OSO_2{}^{14}NH_2$ or $Cl_3CCH_2OSO_2{}^{15}NH_2$ (4); 10^{-2} M] and oxidant **3** [$PhI(O_2CCH_3)_2$ or $PhI(O_2CC(CH_3)_3)_2$; 10^{-1} M] in anhydrous CH_2Cl_2 was directed at a mixture of $Rh_2(esp)_2$ **1** and adamantane (10 μL 10^{-2} M solution of each component in anhydrous CH_2Cl_2 deposited on a paper surface). The resulting DESI-MS spectrum (Fig. 3) shows ions for the Rh catalyst corresponding to $[\mathbf{1}]^+$ and $[\mathbf{1}+Na]^+$ as well as sodiated adduct ions of **2**, **3**, $[\mathbf{3}+\mathbf{3}+Na]^+$ (m/z = 666.9280; quoted m/z values represent the most intense isotope peak of the distribution), and **4**. Sodium ion adducts are common in MS and appear regardless of whether the analyte is deposited on paper or glass. Multiple charged species were not observed in acquired mass spectra. When adamantane is premixed with **1** and then sprayed with a nebulized solution of **2** and **3**, the product sulfonamide **7** is detected at m/z 383.9959 $[\mathbf{7}+Na]^+$ (Fig. 3 and Fig. S1). Fig. S1 shows experimental (background is subtracted; black) and calculated (red) mass spectra of $[\mathbf{2}+Na]^+$ (Fig. S1*A*), $[\mathbf{4}+Na]^+$ (Fig. S1*B*), and $[\mathbf{7}+Na]^+$ (Fig. S1*C*). Although the intensity of $[\mathbf{7}+Na]^+$ is low, its appearance is consistent with the catalytic pathway that we and others have postulated for the C–H amination process (7–9). Many of the ionic

Author contributions: R.H.P., T.J.C., J.L.R., J.D.B., and R.N.Z. designed research; R.H.P. and T.J.C. performed research; J.L.R. contributed new reagents/analytic tools; R.H.P., T.J.C., and J.L.R. analyzed data; and R.H.P., T.J.C., J.L.R., J.D.B., and R.N.Z. wrote the paper.

The authors declare no conflict of interest.

*This Direct Submission article had a prearranged editor.

[1]R.H.P. and T.J.C. contributed equally to this work.

[2]To whom correspondence may be addressed. E-mail: jdubois@stanford.edu or zare@stanford.edu.

This article contains supporting information online at www.pnas.org/lookup/suppl/doi:10.1073/pnas.1207600109/-/DCSupplemental.

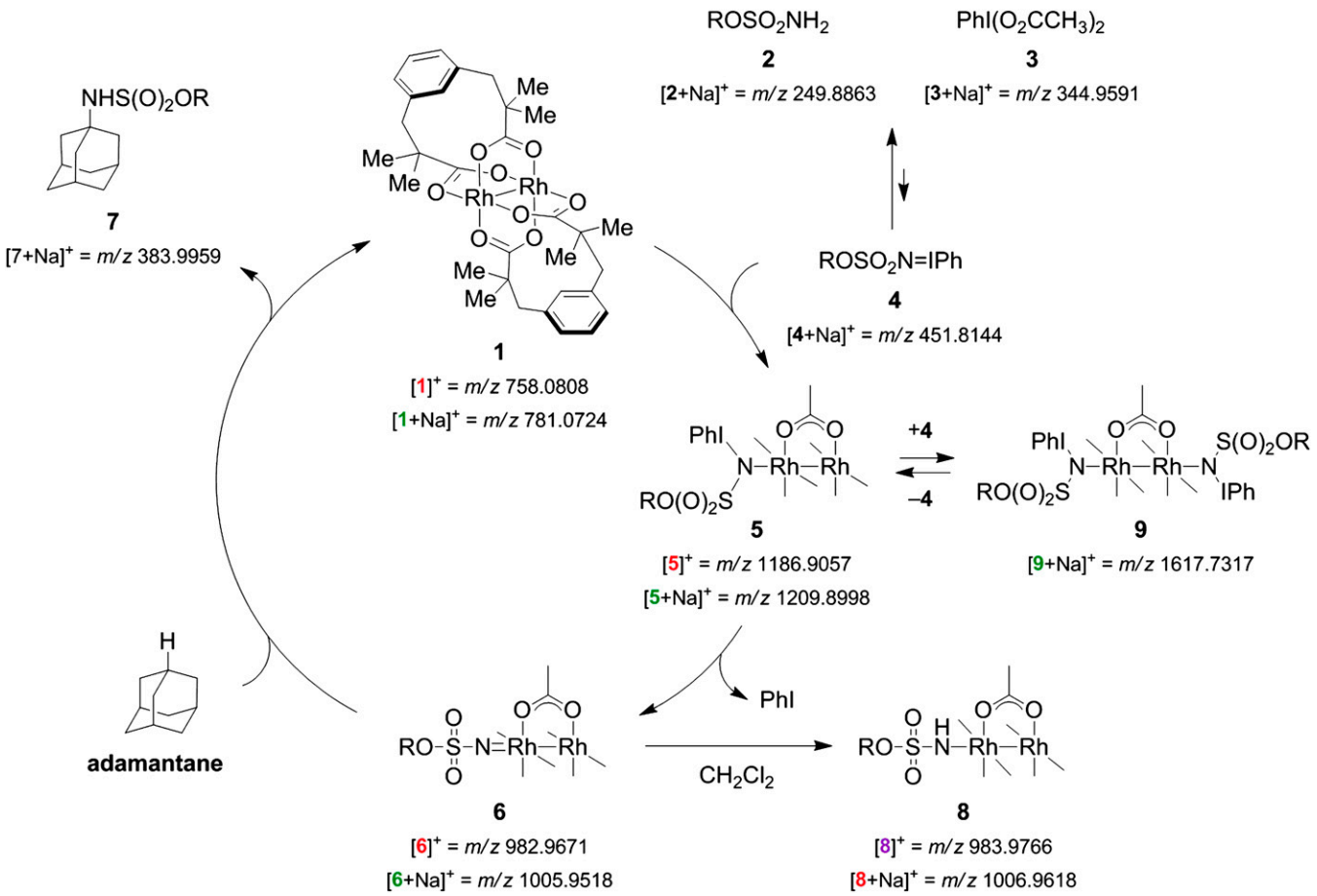

Fig. 1. Proposed mechanism for $Rh_2(esp)_2$-catalyzed C–H amination (R = CH_2CCl_3). The specific ionic species and experimental *m/z* values are shown below each structure. Each experimental *m/z* value is within 5 ppm of the calculated value, which is well within the uncertainty of the LTQ Velos Orbitrap mass spectrometer. The Rh^{2+}/Rh^{2+}, Rh^{2+}/Rh^{3+}, and Rh^{3+}/Rh^{3+} species are shown in green, red, and purple, respectively.

species detected in this study have been proposed previously based on bulk solution mechanistic data. The ability to draw parallels between DESI-MS experiments and the catalytic process is supported by these findings as well as prior studies showing that DESI-MS transfers intact molecules from solution to the gas phase (17, 33).

DESI-MS also reveals a number of intermediate species not previously detected by other analytical methods We have verified the formation of the iminoiodinane–Rh complex, $[[Rh_2(esp)_2]\bullet PhINSO_2OR]^+$ ($[\mathbf{5}]^+$) and $[[Rh_2(esp)_2]\bullet PhINSO_2OR+Na]^+$ ($[\mathbf{5}+Na]^+$), as signals corresponding to *m/z* 1,186.9057 and *m/z* 1,209.8979. High mass accuracy measurements, agreement between calculated and experimental isotopic distributions, and observation of a 1-Da shift for ^{15}N-labeled sulfamate **2** (Fig. 4 *A–D*) provide strong support for these assignments. We did not observe $[\mathbf{5}]^+$ or $[\mathbf{5}+Na]^+$ in continuous flow electrospray ionization (ESI) MS experiments with a reaction time of a few seconds, suggesting that the lifetime of this species is much shorter. Although analogous iminoiodinane–metal complexes have been proposed, only one report documents the ESI-MS detection of a related species, a porphyrin manganese•$PhINSO_2C_6H_4CH_3$ adduct (12, 13, 34). In addition to identifying **5**, a second principal peak is observed at *m/z* 1,080.0535 and is assigned as the coordination complex between catalyst and oxidant $[[Rh_2(esp)_2]\bullet PhI(O_2CCH_3)_2]^+$ ($[\mathbf{1}\bullet\mathbf{3}]^+$) (Fig. S2); $[[Rh_2(esp)_2]\bullet PhI(O_2CC(CH_3)_3)_2]^+$ is also detected at *m/z* 1,164.1449 (Fig. S3) when $PhI(O_2CC(CH_3)_3)_2$ is used as the oxidant. The formation of these species is not surprising given the propensity of dirhodium tetracarboxylate complexes to bind axial ligands and the presence of substantial amounts of the unreacted iodine oxidants.

Structural assignments of the *m/z* 1,186.9057 signal as $[\mathbf{5}]^+$ and the *m/z* 1,080.0535 signal as $[\mathbf{1}\bullet\mathbf{3}]^+$ are supported by the close correspondence of predicted and experimental isotope profiles (Fig. 4*C* and Fig. S2) as well as fragmentation patterns in high-resolution multistage MS (MS^n) experiments (Fig. S4). Dissociation of $[\mathbf{5}]^+$ and $[\mathbf{1}\bullet\mathbf{3}]^+$ yields fragment ions with *m/z* 758.0831 and *m/z* 776.0936, which correspond to $[\mathbf{1}]^+$ and $[\mathbf{1}\bullet H_2O]^+$ (Fig. S4*A*). The water coordination complex $[\mathbf{1}\bullet H_2O]^+$ is also observed in single-stage mass spectra. Dissociation of $[\mathbf{1}\bullet H_2O]^+$ in the MS^2 spectra of $[\mathbf{5}]^+$ and $[\mathbf{1}\bullet\mathbf{3}]^+$ yields $[\mathbf{1}\bullet H]^+$ (Fig. S4*B*), and subsequent collisional activation produces sequential losses of *m/z* 44 and *m/z* 46, which correspond to neutral losses of CO_2 and $[H_2O + CO]$ (35), respectively, from the carboxylate ligands of **1** (Fig. S4*C*). These fragmentation patterns confirm the assignment of *m/z* 1,186.9057 and *m/z* 1,080.0535 as $[\mathbf{5}]^+$ and $[\mathbf{1}\bullet\mathbf{3}]^+$, respectively. Our conclusions are also supported by experiments with $ROSO_2{}^{15}NH_2$, which gives a 1-Da increase for complex $[\mathbf{5}]^+$ to *m/z* 1,187.9041 (Fig. 4*D*) but does not alter the mass of $[\mathbf{1}\bullet\mathbf{3}]^+$.

In addition to $[\mathbf{5}]^+$, an *m/z* corresponding to the bis-ligated species $[\mathbf{9}]^+$ (*m/z* 1,617.7317) is also recorded (Fig. 3). This complex is suspected to be in equilibrium with **5** and is off the previously proposed catalytic path. Dissociation of $[\mathbf{9}]^+$ yields $[\mathbf{5}]^+$ in MS^2 spectra (Fig. S4*D*), supporting its assignment. Other species that were observed include $[\mathbf{5}\bullet\mathbf{3}]^+$ (*m/z* 1,508.8716) and two complexes with PhI=O at *m/z* 1,299.9911 $[\mathbf{1}\bullet\mathbf{3}\bullet PhI{=}O]^+$ and *m/z* 1,406.8474 $[\mathbf{5}\bullet PhI\bullet PhI{=}O]^+$.

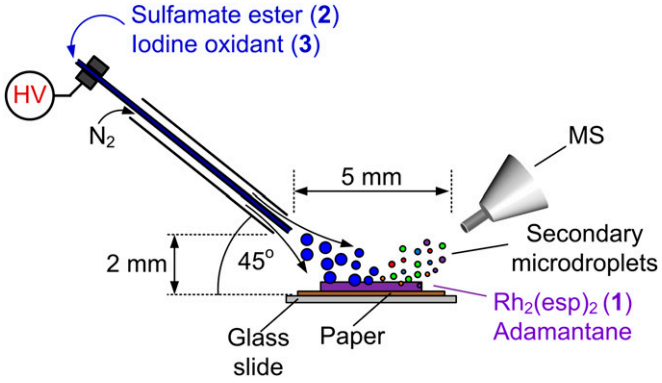

Fig. 2. DESI-MS setup for intercepting transient intermediates of the $Rh_2(esp)_2$-catalyzed C–H amination of adamantane.

Loss of PhI from **5** is believed to generate a reactive Rh-nitrene complex **6** capable of oxidizing C–H bonds. Using DESI-MS, we have directly detected the Rh-nitrene as $[\mathbf{6}+Na]^+$ at *m/z* 1,005.9554 (Fig. 4*E*). The MS profile for $[\mathbf{6}+Na]^+$ (*m/z* 1,005.9554) overlaps with the isotope distribution for another species, which we have identified as $[\mathbf{8}+Na]^+$ (*m/z* 1,006.9618). The resolution at nominal *m/z* 1,006 is ~55,000, which is insufficient to separate the isotopic patterns of these two species. Calculated mass spectra show that $[\mathbf{6}+Na]^+$ and $[\mathbf{8}+Na]^+$ have a ratio of 1:2 for the spectrum displayed in Fig. 4*E*. In addition to the sodiated adducts of **6** and **8**, we also observe signals for $[\mathbf{6}]^+$ (*m/z* 982.9671) and $[\mathbf{8}]^+$ (*m/z* 983.9766) with a calculated ratio of 7:1 (Fig. 4*G* and Fig. S5). The assignments of the $[\mathbf{6}+Na]^+/[\mathbf{8}+Na]^+$ (Fig. S6) and $[\mathbf{6}]^+/[\mathbf{8}]^+$ (Fig. 4*H*) overlapping isotope distributions are confirmed by experiments using $ROSO_2{}^{15}NH_2$, which clearly show the expected 1-Da shifts. DESI-MS experiments performed in CH_2Cl_2 detect $[\mathbf{6}+Na]^+/[\mathbf{8}+Na]^+$ and $[\mathbf{6}]^+/[\mathbf{8}]^+$, irrespective of whether adamantane is present. Importantly, increasing the amount of substrate (adamantane or adamantane carboxylic acid) relative to $Rh_2(esp)_2$ results in an increase in the abundance of the sulfonamide product, with a concomitant decrease in the abundance of the $[\mathbf{6}+Na]^+/[\mathbf{8}+Na]^+$ distribution[†] (Figs. S7 and S8). These results provide additional support for the claim that the detected ionic species are relevant to the bulk solution reaction.

We have used DESI-MS to gain additional insights into the reactivity of the Rh-nitrene complex **6**. Acquired high-resolution DESI-MS spectra reveal two unique Rh^{2+}/Rh^{3+} derivatives, which are assigned as $[Rh_2(esp)_2NHSO_2OR+Na]^+$ ($[\mathbf{8}+Na]^+$ (*m/z* 1,006.9618) (Fig. 4*E*) and $[Rh_2(esp)_2Cl_2]^-$ (*m/z* 828.0225) (Fig. S9). Of these mixed valence species, only **8** is observed within the first few milliseconds of the reaction. A signal for the Rh^{2+}/Rh^{3+} dichloride adduct is detected after incubating the reaction mixtures for several hours. These same experiments show $[\mathbf{8}+Na]^+$ but not the short-lived nitrenoid $[\mathbf{6}+Na]^+$ (Fig. S10). This observation provides additional support for the proposed peak assignments and the estimated lifetimes of these reactive species. From these data, we surmise that complex **8** forms rapidly through hydrogen atom abstraction from the CH_2Cl_2 solvent and competes with the formation of the sulfonamide product **7**.

By conducting DESI-MS experiments in CD_2Cl_2, we have confirmed that $[\mathbf{8}+Na]^+$ results from hydrogen atom abstraction of CH_2Cl_2, which has a measured bond dissociation energy (C–H BDE) of 95.7 kcal/mol (C–H bridgehead BDE of adamantane is 96.2 kcal/mol) (36). In these experiments, there is a 1-Da mass shift corresponding to deuterium incorporation, clearly establishing that $[Rh_2(esp)_2NDSO_2OR]^+$ and $[Rh_2(esp)_2NDSO_2OR+Na]^+$ form as a result of CD_2Cl_2 oxidation (Fig. 4 *E* and *F*). In Fig. 4 *E* and *F*, the $[\mathbf{6}+Na]^+$ to $[\mathbf{8}+Na]^+$ ratio changes from 1:2 to 3:1 when CD_2Cl_2 is used as the solvent, which might be interpreted as evidence of an isotope effect. An accurate estimation of KIE using DESI-MS is not possible, however, due to variations in the $[6+Na]^+$ to $[8+Na]^+$ ratio stemming from low signal intensity as well as difficulties controlling the reaction environment, composition of the microdroplet reaction vessels, and reaction time.

The observation of two nitrenoid species, **6** (detected ion is $[\mathbf{6}+Na]^+$) and $[\mathbf{6}]^+$, that differ in oxidation state raises the intriguing possibility of two catalytically operative pathways for C–H amination. At this time, we can conclude that either **6** or $[\mathbf{6}]^+$ or both **6** and $[\mathbf{6}]^+$ are capable of acting as a one-electron oxidant for C–H abstraction of CH_2Cl_2 solvent. As mixed valent Rh^{2+}/Rh^{3+} species have been identified under standard operating conditions of the intermolecular C–H amination reaction, the involvement of **6** and $[\mathbf{6}]^+$ in solution-phase chemistry is plausible and may explain observed reactivity trends (4, 5, 11).

To avoid solvent oxidation, we have investigated the amination reaction in benzene (C–H BDE ~ 113 kcal/mol) (36). In DESI-MS experiments both with and without adamantane, no signals associated with nitrenoid **6** or **8** are observed. Other coordination adducts, such as $[\mathbf{5}]^+$ and $[\mathbf{1{\bullet}3}]^+$, along with sulfonamide **7** appear in accordance with results from the CH_2Cl_2 experiments. No products of benzene amination (e.g., aniline or azepine) have been detected. If adamantane oxidation is occurring through hydrogen atom abstraction rather than a concerted insertion event, we conclude that the subsequent radical rebound reaction to form **7** is sufficiently fast to outcompete diffusion of **8** from the solvent cage. Alternatively, the stability and lifetime of **6** and **8** may differ between solvents. In addition, differing conditions in the secondary microdroplets compared with bulk solutions could lead to different reaction outcomes and kinetics (37); however, we have not observed any ionic species indicating that the mechanism of C–H amination occurring in the microdroplets differs from bulk solution.

The identification of short-lived reactive intermediates using DESI-MS enhances our mechanistic understanding of the Rh-catalyzed C–H amination reaction. We have obtained high-resolution MS data for species that are generally regarded to be intermediates in the catalytic pathway for this process. In addition, our experiments suggest that both a dirhodium iminoiodinane adduct **5** and a dirhodium nitrene **6** are generated transiently and that the nitrenoid species can function as a one-electron oxidant for hydrogen atom abstraction (4, 5, 11). The identification of two Rh-nitrene adducts differing in oxidation state (**6**, detected by $[\mathbf{6}+Na]^+$, and $[\mathbf{6}]^+$) is arguably one of the most revealing

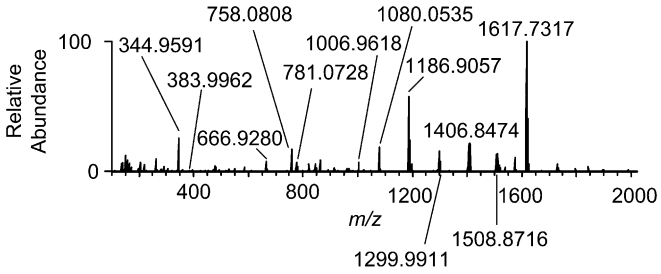

Fig. 3. DESI mass spectrum showing reaction intermediates formed in $Rh_2(esp)_2$-catalyzed C–H amination of adamantane (Fig. S1 shows zoomed in spectra for $[\mathbf{2}+Na]^+$, $[\mathbf{4}+Na]^+$, and $[\mathbf{7}+Na]^+$).

[†]We also noted that, at higher adamantane and adamantane carboxylic acid concentrations, the intensity of the sulfonamide product does not increase appreciably, suggesting that both the extraction rate from the surface and substrate solubility limit the concentration of analyte in the secondary microdroplets. The signal intensity is very low for the sulfonamide products of adamantane and adamantane carboxylic acid, leading to variability of measurement. However, consistent qualitative trends in signal intensity as a function of substrate loading are observed for both adamantane and adamantane carboxylic acid.

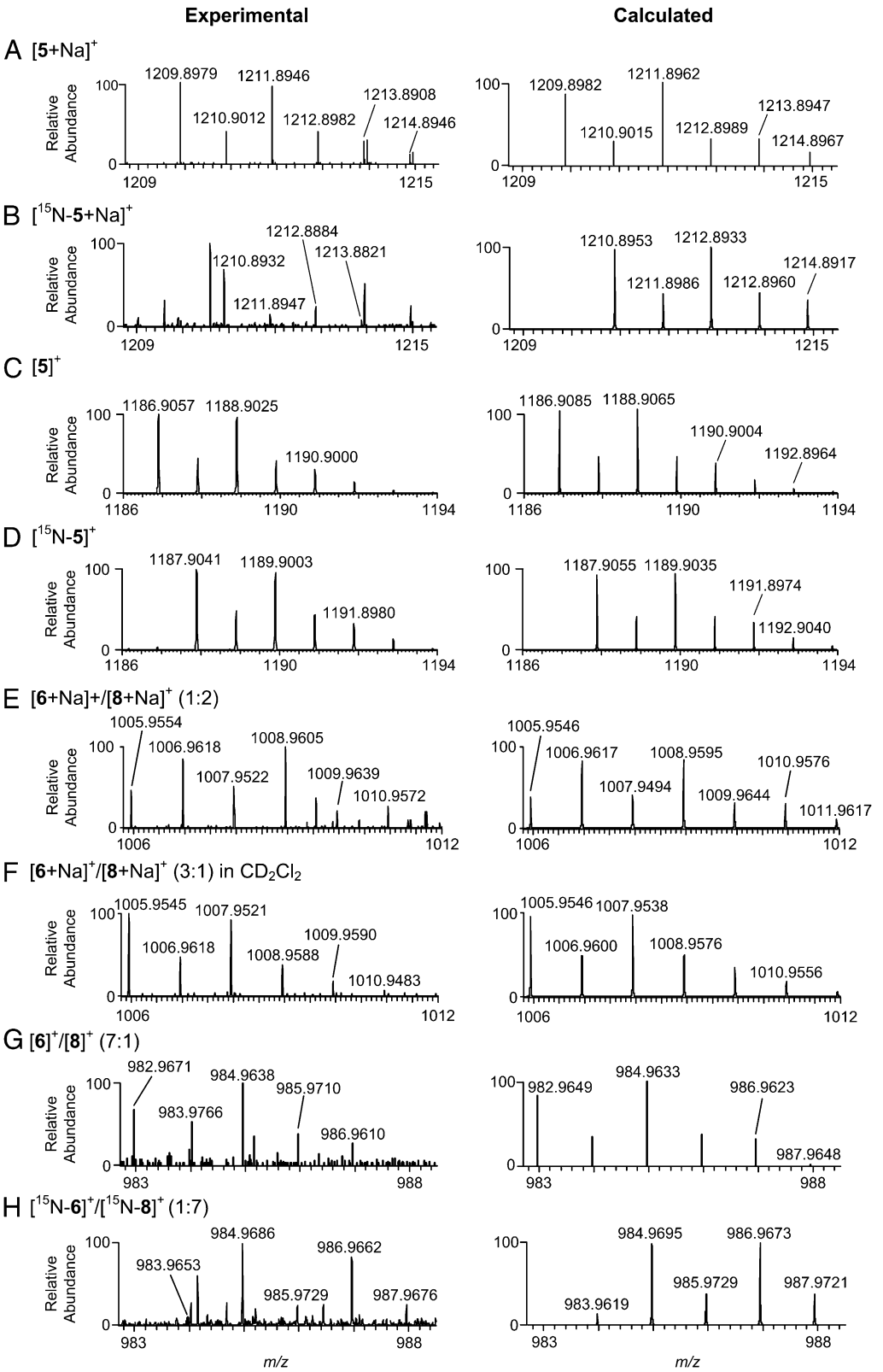

Fig. 4. Experimental and calculated mass spectral isotope profiles. *A* and *C* show spectra for [**5**+Na]$^+$ and [**5**]$^+$ produced using $ROSO_2{}^{14}NH_2$; corresponding spectra using $ROSO_2{}^{15}NH_2$ are shown in *B* and *D*. *E* and *G* show spectra for the overlapping isotope distributions of [**6**+Na]$^+$/[**8**+Na]$^+$ (calculated ratio of 1:2) and [**6**]$^+$/[**8**]$^+$ (calculated ratio of 7:1) for $ROSO_2{}^{14}NH_2$. *F* shows overlapping signals of [**6**+Na]$^+$/[**8**+Na]$^+$ in CD_2Cl_2 (calculated [**6**+Na]$^+$ to [**8**+Na]$^+$ ratio of 3:1). *H* shows overlapping signals from [**6**]$^+$ and [**8**]$^+$ (1:7) using $ROSO_2{}^{15}NH_2$. Signal intensities for the [**6**]$^+$/[**8**]$^+$ distributions (*G* and *H*) are very low. Therefore, for clarity, ion signals that were larger than the isotope signals from [**6**]$^+$/[**8**]$^+$ were subtracted, and the spectrum was normalized to the most intense signal from [**6**]$^+$/[**8**]$^+$. The complete mass spectra for *G* and *H* are shown in Fig. S5.

discoveries and provides an experimental clue that more than one discrete mechanism may function for C–H amination. These results underscore the power of DESI-MS as an analytical method for mechanistic inquiry of fast reaction processes that should substantially impact efforts in catalytic reaction methods development.

Methods

Materials. Unless specified otherwise, all chemicals were purchased from Sigma-Aldrich and used without additional purification. The synthesis of isotopically labeled 2,2,2-trichloroethylsulfamate **2** ($Cl_3CCH_2OSO_2{}^{15}NH_2$) is described in ref. 4.

DESI-MS. A solution of trichloroethylsulfamate **2** ($Cl_3CCH_2OSO_2{}^{14}NH_2$ or $Cl_3CCH_2OSO_2{}^{15}NH_2$; 10^{-2} M) and oxidant **3** [$PhI(O_2CCH_3)_2$ or $PhI(O_2CC(CH_3)_3)_2$; 10^{-1} M] in an anhydrous solvent (CH_2Cl_2, CD_2Cl_2, C_6H_6, or C_6D_6) was infused through the fused silica capillary tubing (100 μm i.d., 360 μm o.d.) of a custom DESI source (20) at a rate of 50 μL/min (0 or 5 kV spray voltage). An N_2 sheath gas (0.6 $Lmin^{-1}$) generated a microdroplet spray that was directed at a paper surface onto which a solution containing **1** (10^{-2} M) and adamantane (one and five equivalents) in anhydrous CH_2Cl_2 was deposited (10 μL). The secondary microdroplets from the surface were sampled by an LTQ Velos Orbitrap mass spectrometer (Thermo Fisher Scientific). Instrument settings were as follows: ion transfer capillary temperature = 200 °C; *m/z* resolution = 100,000 at *m/z* 400; single-stage MS scan range = *m/z* 150 − *m/z* 2,000; for MS^n experiments, normalized collision energy = 30%. For experiments that involve reaction times of several hours, the reagents were mixed in a borosilicate vial and then analyzed by DESI-MS using a dichloromethane (anhydrous) microdroplet spray. Continuous-flow ESI-MS experiments were carried by infusing two solutions (10 μL/min) into a static mixing tee (IDEX Health & Science). The PEEK tubing connected to the outlet of the mixing tee was connected to an ESI source. The length of the outlet tubing set a reaction time of a few seconds before ESI-MS analysis.

ACKNOWLEDGMENTS. We thank Pavel Aronov, Randall Mann, and Allis Chien (Stanford University Mass Spectrometry) for providing instrumentation and their expertise in the field of MS. We also thank Ali Ismail and Nick K. Davis for technical help with the experiments. Financial support from Air Force Office of Scientific Research Grant FA 9550-10-1-0235 and the National Science Foundation Center for Stereoselective C–H Functionalization (CSCHF) is gratefully acknowledged. R.H.P. thanks the Center for Molecular Analysis and Design at Stanford University (1123893-1-AABGE). T.J.C. acknowledges the Department of Defense for a National Defense and Science Engineering Graduate Research Fellowship. J.L.R. thanks the National Institutes of Health for Fellowship 5F32GM089033-02.

1. Zalatan DN, Du Bois J (2010) *Metal-Catalyzed Oxidations of C-H to C-N Bonds. Topics in Current Chemistry, C-H Activation*, eds Yu JQ, Shi Z (Springer-Verlag, Berlin), Vol 292, pp 347–378.
2. Davies HML, Manning JR (2008) Catalytic C-H functionalization by metal carbenoid and nitrenoid insertion. *Nature* 451(7177):417–424.
3. Best SP, Nightingale AJ, Tocher DA (1991) The destructive oxidation of a rhodium(II) dimer—Crystal and molecular structure of $[Rh(Ph)(SbPh_3)_2Cl_2(CH_3CN)]$. *Inorganica Chim Acta* 181:7–9.
4. Fiori KW, Du Bois J (2007) Catalytic intermolecular amination of C-H bonds: Method development and mechanistic insights. *J Am Chem Soc* 129(3):562–568.
5. Zalatan DN, Du Bois J (2009) Understanding the differential performance of $Rh_2(esp)_2$ as a catalyst for C-H amination. *J Am Chem Soc* 131(22):7558–7559.
6. Doyle MP, Duffy R, Ratnikov M, Zhou L (2010) Catalytic carbene insertion into C-H bonds. *Chem Rev* 110(2):704–724.
7. Fiori KW, Espino CG, Brodsky BH, Du Bois J (2009) A mechanistic analysis of the Rh-catalyzed intramolecular C-H amination reaction. *Tetrahedron* 65:3042–3051.
8. Huard K, Lebel H (2008) N-Tosyloxycarbamates as reagents in rhodium-catalyzed C-H amination reactions. *Chemistry* 14(20):6222–6230.
9. Müller P, Baud C, Naegeli I (1998) Rhodium(II)-catalyzed nitrene transfer with phenyliodonium ylides. *J Phys Org Chem* 11:597–601.
10. Nakamura E, Yoshikai N, Yamanaka M (2002) Mechanism of C-H bond activation/C-C bond formation reaction between diazo compound and alkane catalyzed by dirhodium tetracarboxylate. *J Am Chem Soc* 124(24):7181–7192.
11. Kornecki KP, Berry JF (2011) Evidence for a one-electron mechanistic regime in dirhodium-catalyzed intermolecular C-H amination. *Chemistry* 17(21):5827–5832.
12. Lin XF, Sun JA, Xi YY, Pang B (2011) Computational interpretation of the stereoselectivity for a dirhodium tetracarboxylate-catalyzed amidation reaction. *Comput Theor Chem* 963:284–289.
13. Lin XF, Zhao CY, Che CM, Ke ZF, Phillips DL (2007) A DFT study on the mechanism of Rh_2(II,II)-catalyzed intramolecular amidation of carbamates. *Chem Asian J* 2(9):1101–1108.
14. Espino CG, Du Bois J (2001) A Rh-catalyzed C-H insertion reaction for the oxidative conversion of carbamates to oxazolidinones. *Angew Chem Int Ed Engl* 40(3): 598–600.
15. Yu XQ, Huang JS, Zhou XG, Che CM (2000) Amidation of saturated C-H bonds catalyzed by electron-deficient ruthenium and manganese porphyrins. A highly catalytic nitrogen atom transfer process. *Org Lett* 2(15):2233–2236.
16. Cooks RG, et al. (2011) New ionization methods and miniature mass spectrometers for biomedicine: DESI imaging for cancer diagnostics and paper spray ionization for therapeutic drug monitoring. *Faraday Discuss* 149:247–267.
17. Cooks RG, Ouyang Z, Takats Z, Wiseman JM (2006) Detection Technologies. Ambient mass spectrometry. *Science* 311(5767):1566–1570.
18. Takáts Z, Wiseman JM, Cooks RG (2005) Ambient mass spectrometry using desorption electrospray ionization (DESI): Instrumentation, mechanisms and applications in forensics, chemistry, and biology. *J Mass Spectrom* 40(10):1261–1275.
19. Takáts ZW, Wiseman JM, Gologan B, Cooks RG (2004) Mass spectrometry sampling under ambient conditions with desorption electrospray ionization. *Science* 306(5695): 471–473.
20. Perry RH, et al. (2012) Transient Ru-methyl formate intermediates generated with bifunctional transfer hydrogenation catalysts. *Proc Natl Acad Sci USA* 109(7):2246–2250.
21. Perry RH, Splendore M, Chien A, Davis NK, Zare RN (2011) Detecting reaction intermediates in liquids on the millisecond time scale using desorption electrospray ionization. *Angew Chem Int Ed Engl* 50(1):250–254.
22. Johansson JR, Nordén B (2012) Sniffing out early reaction intermediates. *Proc Natl Acad Sci USA* 109(7):2186–2187.
23. Hu QZ, et al. (2005) The Orbitrap: A new mass spectrometer. *J Mass Spectrom* 40(4): 430–443.
24. Perry RH, Cooks RG, Noll RJ (2008) Orbitrap mass spectrometry: Instrumentation, ion motion and applications. *Mass Spectrom Rev* 27(6):661–699.
25. Roithová J (2012) Characterization of reaction intermediates by ion spectroscopy. *Chem Soc Rev* 41(2):547–559.
26. Espy RD, Badu-Tawiah A, Cooks RG (2011) Analysis and modification of surfaces using molecular ions in the ambient environment. *Curr Opin Chem Biol* 15(5):741–747.
27. Xu GM, Chen B, Guo B, He DX, Yao SZ (2011) Detection of intermediates for the Eschweiler-Clarke reaction by liquid-phase reactive desorption electrospray ionization mass spectrometry. *Analyst (Lond)* 136(11):2385–2390.
28. Coelho F, Eberlin MN (2011) The bridge connecting gas-phase and solution chemistries. *Angew Chem Int Ed Engl* 50(23):5261–5263.
29. Desikan V, Liu Y, Toscano JP, Jenks WS (2008) Photochemistry of N-acetyl-, N-trifluoroacetyl-, N-mesyl-, and N-tosyldibenzothiophene sulfilimines. *J Org Chem* 73 (12):4398–4414.
30. Garay J-C, Maloney V, Marlow M, Small P (1996) Spectroscopy and kinetics of triplet 4-methylbenzenesulfonylnitrene. *J Phys Chem* 100:5788–5793.
31. Gritsan NP, Platz MS (2006) Kinetics, spectroscopy, and computational chemistry of arylnitrenes. *Chem Rev* 106(9):3844–3867.
32. Yurkovich MJ, et al. (2009) The reactivity of metallated nitrenium ions studied by FT-ICR. *Int J Mass Spectrom* 287:16–20.
33. Ifa DR, Wu CP, Ouyang Z, Cooks RG (2010) Desorption electrospray ionization and other ambient ionization methods: Current progress and preview. *Analyst (Lond)* 135(4):669–681.
34. Zhou XG, Yu XQ, Huang JS, Che CM (1999) Asymmetric amidation of saturated C-H bonds catalysed by chiral ruthenium and manganese porphyrins. *Chem Commun*, 10.1039/A907653K.
35. Benoit F, Holmes JL (1972) Mass spectra of carboxylic acids. 4. Carboxyl-carboxyl interaction in some cycloalkane 1,2 dicarboxylic acids and its relationship with molecular geometry. *Org Mass Spectrom* 6:541–548.
36. Luo Y-R (2007) *Comprehensive Handbook of Chemical Bond Energies* (Taylor & Francis, Boca Raton, FL).
37. Girod M, Moyano E, Campbell DI, Cooks RG (2011) Accelerated bimolecular reactions in microdroplets studied by desorption electrospray ionization mass spectrometry. *Chem Sci* 2:501–510.